ORIGINAL SCIENTIFIC PAPER

CROATICA CHEMICA ACTA

Croat. Chem. Acta **2025**, *98*(3), 215–222
Published online: December 30, 2025
DOI: 10.5562/cca4204

HKD 1926

A Novel Tris(Chromium(III))–4-Nitrocatechol Complex Extracted via an Eco-Friendly Ionic Liquid-Assisted Method

Petya Vassileva Racheva,[1] Antoaneta Dimitrova Saravanska,[1] Denitsa Dimitrova Kiradzhiyska,[1,2] Vassil Borisov Delchev,[3] Kiril Blazhev Gavazov[1,*]

[1] Department of Chemical Sciences, Medical University of Plovdiv, 120 Buxton Brothers St., Plovdiv 4004, Bulgaria
[2] Research Institute at the Medical University of Plovdiv, 15A Vasil Aprilov Bld., Plovdiv, Bulgaria
[3] Department of Physical Chemistry, Faculty of Chemistry, Plovdiv University "Paisii Hilendarski", 24 Tsar Assen Street, Plovdiv 4000, Bulgaria
* Corresponding author's e-mail address: kiril.gavazov@mu-plovdiv.bg

RECEIVED: September 22, 2025 ✶ REVISED: October 23, 2025 ✶ ACCEPTED: October 29, 2025

Abstract: A novel mixed-micelle-mediated cloud point extraction (MM-CPE) system for Cr(III) was investigated spectrophotometrically. In this system, 4-nitrocatechol (4NC) acts as the chelating agent, while the ionic liquid Aliquat 336 (A336) functions both as a cationic ion-association reagent and as a co-surfactant that forms mixed micelles with Triton X-114. The extracted complex was identified as $(A336^+)_3[Cr(4NC)_3]$. The structure of its anionic part $[Cr(4NC)_3]^{3-}$ was further analyzed through B3LYP/6-311G theoretical optimizations and by comparing calculated and experimental UV/Vis spectra. The ternary complex exhibits a maximum absorbance at 475 nm with a molar absorption coefficient of 2.4×10^5 M^{-1} cm^{-1} (tenfold enrichment). The calibration curve demonstrated linearity over a Cr(III) concentration range of 40–420 ng mL^{-1}, with a detection limit of 12 ng mL^{-1}. The logarithmic conditional extraction constant (K_{ex}) was determined to be 12.0 ± 0.1, indicating an efficient extraction process.

Keywords: chromium(III), cloud point extraction, spectrophotometry, 4-nitrobenzene-1,2-diol, Aliquat336, TD DFT calculations.

INTRODUCTION

CHROMIUM is a hard, brittle, and corrosion-resistant metal with widespread industrial and technological applications. It is the primary alloying element in stainless steel production and ranks 21st in abundance within the Earth's lithosphere. To date, approximately 110 chromium-bearing minerals have been documented,[1] with chromium occurring in several oxidation states. Among these, Cr(III) and Cr(VI) are the most prevalent and environmentally relevant due to their contrasting stability, mobility, and toxicity.[2–4] Chromium(VI) is of particular concern due to its well-established carcinogenicity,[4,5] whereas Cr(III) has traditionally been regarded as an essential trace element in human nutrition.[6–8]

Cr(III) supplementation has been linked to improved glucose metabolism, mitigation of metabolic and polycystic ovary syndromes, modulation of dyslipidemia, and changes in body weight and lean mass. Evidence for these effects, however, remains inconsistent and controversial.[9–12] In 2014, the Panel on Dietetic Products, Nutrition and Allergies (NDA) of the European Food Safety Authority (EFSA) evaluated the available data on chromium intake and concluded that no beneficial effects could be substantiated in healthy individuals.[12]

Cr(III) can be produced by dissolving elemental chromium in acids or by reducing Cr(VI) compounds, with interconversion possible under certain conditions.[11,13,14] This duality contributes to the ongoing debate over whether chromium should be regarded as an essential element, a pharmacologically active agent, or a toxicant.[15]

Chromium(III) adopts a d^3 electron configuration, with three electrons occupying the lower-energy t_2g orbitals (d_{xy}, d_{xz}, d_{yz}) in an octahedral crystal field. This electron arrangement results in significant crystal field stabilization and contributes to the overall stability of the complex. As a

result, Cr(III) typically forms octahedral complexes that are both kinetically inert and thermodynamically stable.

Chromium(III) forms chelate complexes with ligands containing oxygen, nitrogen, or sulfur donor atoms.[16–22] In aqueous media, complexation typically requires heating the reaction mixture to elevated temperatures (≥ 80 °C),[22–28] as this promotes efficient ligand exchange and facilitates the formation of Cr(III) chelates—a step generally unnecessary for many other metal ions. Following the formation of the desired Cr(III) complex, conventional liquid–liquid extraction procedures usually involve cooling the mixture before introducing volatile organic solvents such as chloroform, toluene, benzene, or carbon tetrachloride. This cooling step extends the overall analytical process, and the reliance on hazardous solvents raises significant environmental and health concerns, rendering these methods less desirable from a green chemistry perspective.

Cloud point extraction (CPE) has been identified as a highly suitable method for preconcentrating Cr(III) because it replaces toxic, volatile organic solvents with surfactants and requires heating,[29–34] which conveniently aligns with the thermal requirements for efficient chelation.[35–48] An additional advantage of performing Cr(III) complexation in micellar media is the reduced reaction time, which can be attributed to micelles' ability to induce favorable shifts in equilibrium constants.[33,49]

4-Nitrocatechol (4NC) is a well-established analytical reagent.[50–53] It carries a 'green dossier,' meaning its label bears no hazard pictograms or hazard/precautionary statements.[54] Although it forms complexes with more than 40 metal ions,[51] no studies have reported its complexes with chromium.

In our previous studies on mixed micelle–mediated centrifuge-less cloud point extraction (MM-CL-CPE) of vanadium,[55] molybdenum,[56] and copper,[57] we observed that Cr(III) significantly interferes with their spectrophotometric determination. The presence of Cr(III) produced markedly enhanced absorbance signals that were difficult to mask, which piqued our interest and prompted further investigation in this field.

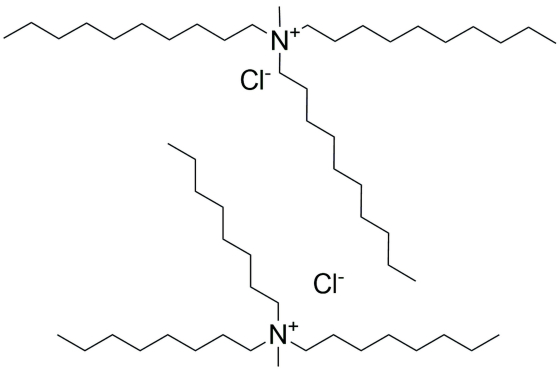

Figure 1. Aliquat 336; the main component of the mixture is trioctylmethylammonium chloride.

The primary objective of this work was to investigate the CPE behavior of Cr(III) in a mixed micellar medium composed of the nonionic surfactant Triton X-114 (TX114) and the ionic liquid Aliquat 336 (A336), a mixture of quaternary ammonium chlorides with an average molar mass of 432 g mol^{-1} (Figure 1).[58] This surfactant system has previously demonstrated effectiveness in the CPE of Mo(VI),[56] Cu(II),[57] and Tl(III).[59] A secondary objective was to employ B3LYP/6-311G calculations to model the color-bearing Cr(III)–4NC chelate and to evaluate its structural parameters.

EXPERIMENTAL SECTION

Reagents and Chemicals

All chemicals were procured from Merck (Schnelldorf, Germany) and utilized without additional purification. A stock solution of Cr(III) (1 mg mL^{-1}) was prepared from $(NH_4)Cr(SO_4)_2 \times 12\,H_2O$,[60] and working solutions (2×10^{-4} M) were obtained by appropriate dilution with water. An aqueous solution of 4NC (≥96.0 %) was prepared at a concentration of 7.5×10^{-3} M. A 10 % (*w* / *w*) aqueous solution of TX114 (laboratory-grade) and a methanol solution of A336 (1×10^{-2} M) were used. Buffer solutions with pH-values ranging from 4.5 to 9.9 were prepared from 2.0 M CH_3COOH and NH_3 solutions. Water was purified by deionization or distillation.

Instrumentation

UV-Vis spectrophotometric measurements were conducted using a Drawell DU-8800RS (Chongqing, China) and an Ultrospec 3300 Pro (Garforth, UK), both equipped with 10 mm macro cuvettes. Mass and pH-values were measured using an Ohaus Pioneer PA214C analytical balance (Parsippany, USA) and a WTW InoLab 7110 pH-meter (Weilheim, Germany), respectively. Heating was carried out using a GFL 1023 water bath (Berlin, Germany).

CPE-Spectrophotometric Optimization

Solutions of TX114, buffer, 4NC, Cr(III), and A336 were combined in 50 mL centrifuge tubes and diluted to volume with water. The mixtures were incubated in a water bath at 50–80 °C for 20–80 minutes, then briefly cooled under running water. The tubes were subsequently placed in a –20 °C freezer for 50 minutes to solidify the surfactant-rich phases (SRPs), facilitating their separation by decantation. Each SRP was then adjusted to a final mass of 5.00 g by adding 0.5 mL of ethanol and a few drops of water, with the mass measured using an analytical balance (by weighing

the empty tubes and then the tubes containing the diluted SRPs). The mixtures were homogenized by shaking and transferred to cuvettes for visible-range absorbance measurements.

THEORETICAL SECTION

The ground-state equilibrium geometry of the proposed anionic chromophore, $[Cr(4NC)_3]^{3-}$, was optimized in the gas phase at the B3LYP/6-311G level of theory without imposing any symmetry or structural constraints. The spin multiplicity and overall charge were set to 4 and −3, respectively. Subsequent frequency calculations confirmed that the optimized structure corresponded to a true minimum, as evidenced by the absence of imaginary frequencies. Vertical excitation energies were then calculated to simulate the UV/Vis spectrum. All computations were carried out using GAUSSIAN 16,[61] and structural visualization was performed with ChemCraft v. 1.8.[62]

RESULTS AND DISCUSSION

Optimal Conditions

The extracted ternary Cr(III)–4NC–A336 complex displays an orange color, with a maximum absorbance at λ = 475 nm, while the blank solution appears yellow. Figure 2 presents the corresponding molecular spectra: (1) the spectrum of the complex measured against the blank, and (2) the spectrum of the blank solution measured against water.

The impact of the pH-value of the buffer solution is illustrated in Figure 3. The analytical signal reaches its maximum at a pH-value of approximately 6.4. All subsequent experiments were therefore carried out at this pH-value, using a buffer volume of 2 mL. Tests performed with different buffer volumes (1–5 mL) indicated that the volume is not a critical parameter: the dependence of absorption on buffer volume within this range is essentially linear, with a slope close to zero (2×10^{-4}).

Figure 4 shows the effect of 4NC and A336 concentrations. The optimal 4NC concentration was determined to be 3.3×10^{-4} M (series 1), achieved by adding 2.2 mL of a 7.5×10^{-3} M solution. The optimal A336 concentration was 2.4×10^{-4} M (series 2), corresponding to 1.2 mL of a 1.0×10^{-2} M A336 solution.

The experimental curve of absorbance versus TX114 mass fraction closely matched those obtained in our previous studies on the Cu(II)–4NC–A336 complex,[57] exhibiting a maximum at 0.4–0.5 % (*w* / *w*). Accordingly, all subsequent experiments in this work were carried out at a TX114 mass fraction of 0.46 %, achieved by adding 2.3 mL of a 10 % TX114 solution.

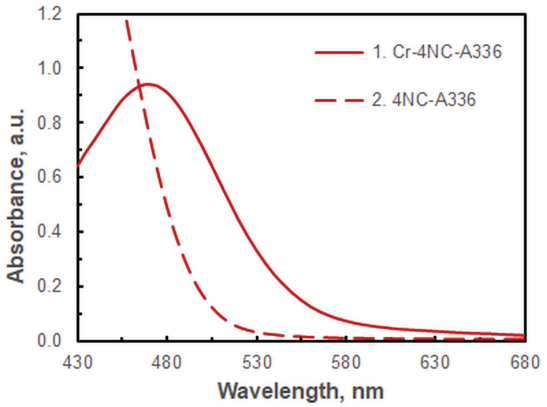

Figure 2. Molecular spectra of the Cr(III)–4NC–A336 complex against blank (1) and the blank solution against water (2). $c_{Cr} = 3.9 \times 10^{-6}$ M, pH = 6.4, $c_{4NC} = 3.3 \times 10^{-4}$ M, $c_{A336} = 2.4 \times 10^{-4}$ M, $w_{TX114} = 0.46$ %, $t_{inc} = 60$ min at 80 °C.

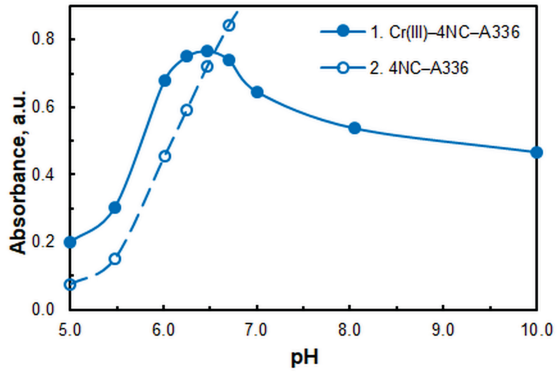

Figure 3. The effect of pH. $c_{Cr} = 3.2 \times 10^{-6}$ M, $c_{4NC} = 3.3 \times 10^{-4}$ M, $c_{A336} = 2.4 \times 10^{-4}$ M, $w_{TX114} = 0.46$ %, $t_{inc} = 60$ min at 80 °C, $\lambda = 475$ nm.

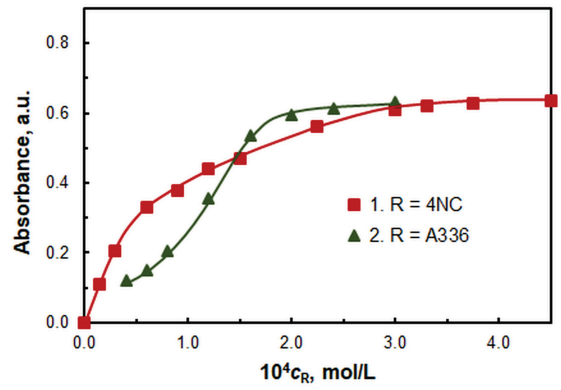

Figure 4. The effect of 4NC (series 1) and A336 (series 2) concentrations. $c_{Cr} = 2.6 \times 10^{-6}$ M, pH = 6.4, $w_{TX114} = 0.46$ %, $t_{inc} = 60$ min at 80 °C, $\lambda = 475$ nm. 1 – $c_{A336} = 2.4 \times 10^{-4}$ M; 2 – $c_{4NC} = 3.3 \times 10^{-4}$ M.

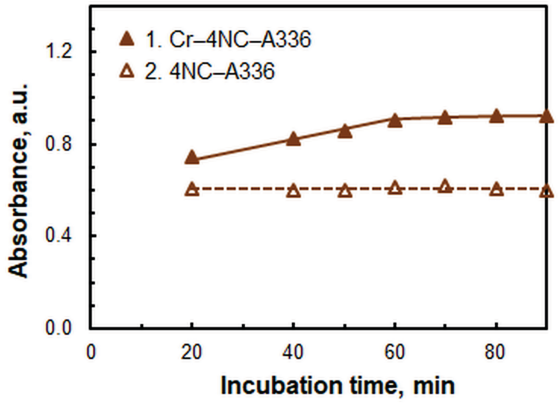

Figure 5. The effect of incubation time. T = 80 °C, pH = 6.4, c_{Cr} = 3.9 × 10^{-6} M, w_{TX114} = 0.46 %, c_{4NC} = 3.3 × 10^{-4} M, c_{A336} = 2.4 × 10^{-4} M, λ = 475 nm.

As noted above, the formation of Cr(III) chelates requires higher temperatures than those typically used for other metal ions. Preliminary temperature-optimization experiments showed that complexation remains incomplete below 80 °C. Under otherwise identical conditions, the absorbance measured at 60 °C was about 14 % lower than at 80 °C, while at 70 °C it was roughly 5 % lower.

Figure 5 illustrates the effect of incubation time at 80 °C. The data indicate that the optimal incubation time is 60 min, measured from the moment the room-temperature samples are placed in the hot water bath. This value is consistent with reported times for other MM-CL-CPE systems using 4NC; for instance, Mo(VI) requires 55 min,[56] while V(V) requires 70 min.[55]

Table 1. The results of the system's optimization

Parameter	Optimal Value
Wavelength, nm	475
pH-value	6.4
Buffer volume, mL	2.0
TX114 mass fraction, %	0.46
4NC concentration, M	3.3 × 10^{-4}
A336 concentration, M	2.4 × 10^{-4}
Incubation temperature, °C	80
Incubation time at 80 °C, min	60
Cooling time at −20 °C, min	50
Test tube capacity, mL	50
Mass[(a)] of the diluted SRP, g	5.00

[(a)] Diluted with C_2H_5OH (0.5 mL) and water.

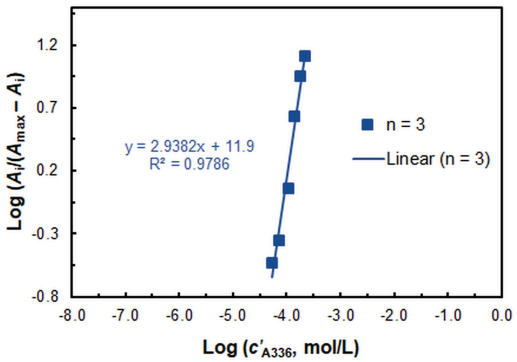

Figure 6. Determination of the A336:Cr(III) molar ratio by the mobile equilibrium method.

A complete set of optimized parameters is presented in Table 1. The cooling time and SRP processing conditions were adopted from experiments reported in previous studies.[55,56] A suitable blank absorbance was achieved by adjusting the mass of the diluted SRP to 5.00 g, which included 0.5 mL of C_2H_5OH added to reduce viscosity.

Stoichiometry and Equation of Complex Formation

The mobile equilibrium method,[63] which is well-suited for analyzing stepwise complexation, was used to determine the molar ratios in the extracted ternary complex. As shown in Figure 6, the molar ratio of A336 to Cr(III) is 3 : 1. There is no evidence of complex formation with any other molar ratio.

In contrast, Figure 7 shows that the molar ratio of 4NC to Cr(III) depends on the 4NC concentration. At $c_{4NC} \leq 1.2 \times 10^{-4}$ M, the ratio is 1 : 1, whereas at $c_{4NC} \geq 1.5 \times 10^{-4}$ M, the ratio shifts to 3 : 1. This behavior is consistent with the expected difficulty of replacing coordinated water molecules in the inert aqua complex $[Cr(H_2O)_6]^{3+}$.

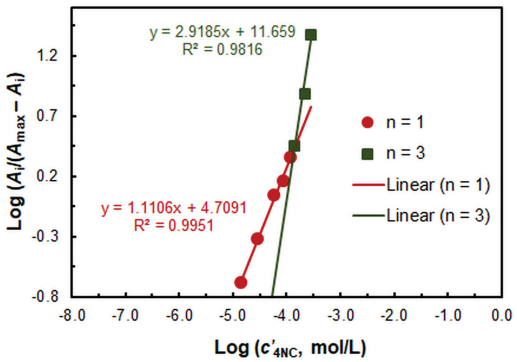

Figure 7. Determination of the 4NC:Cr(III) molar ratios by the mobile equilibrium method.

There is no indication that a stable 2 : 1 (4NC : Cr(III)) intermediate complex forms. Once the threshold concentration of 4NC is reached, it is likely that the remaining water molecules in the inner coordination sphere are rapidly substituted.

The molar ratios determined under optimal conditions support the proposed mechanism of complexation and CPE, as expressed in Equation 1, where H_2L denotes the protonated form of 4NC. This species predominates under the chosen conditions, given that the first pK_a of 4NC is approximately 6.7.[51,64,65]

$$Cr^{3+}(aq) + 3\,H_2L(aq) + 3\,A336^+(aq) \rightleftharpoons (A336)_3[CrL_3](srp) + 6\,H^+ \quad (1)$$

Ground-State Equilibrium Geometry of the Anionic Component. Comparison of Theoretical and Experimental Spectra

The extracted hydrophobic, electrically neutral complex can be regarded as an ionic associate consisting of the anion $[CrL_3]^{3-}$ and three monovalent cations $A336^+$, which together compensate the overall charge (Equation 2):

$$[CrL_3]^{3-} + 3\,A336^+ \rightleftharpoons (A336)_3[CrL_3] \quad (2)$$

In complexes of this type, the absorption bands observed in the visible region are characteristic of the anionic component.[52,53,66–68] Because the full electroneutral complex $(A336)_3[CrL_3]$ contains a large number of atoms, direct modeling of its structure is computationally challenging. A practical approach is to optimize the geometry of the anionic component (chromophore part), compute its theoretical spectrum, and then compare it with the experimental spectrum. A favorable agreement between these spectra (calculated and experimental) would support the proposed structure.

Figure 8 shows the optimized geometry of the anionic moiety $[Cr(4NC)_3]^{3-}$. As expected, the complex adopts an octahedral configuration, with bond angles involving the Cr(III) center and the trans-coordinated oxygen atoms approaching 180°: >O(1)–Cr(43)–O(14) = 171.1°, >O(2)–Cr(43)–O(24) = 172.3°, and >O(3)–Cr(43)–O(13) = 172.9°. However, the $[Cr^{III}(4NC)_3]^{3-}$ complex exhibits a more pronounced distortion from ideal geometry than the octahedral structure of the low-spin $[Fe^{III}(4NC)_3]^{3-}$,[53] which was optimized using the same B3LYP/6-311G method. For example, in the Cr(III) complex, one oxygen atom is displaced by 7.4° from the equatorial plane defined by the other three coordinated oxygens, whereas in the Fe(III) analogue, the corresponding deviation does not exceed 0.6°.

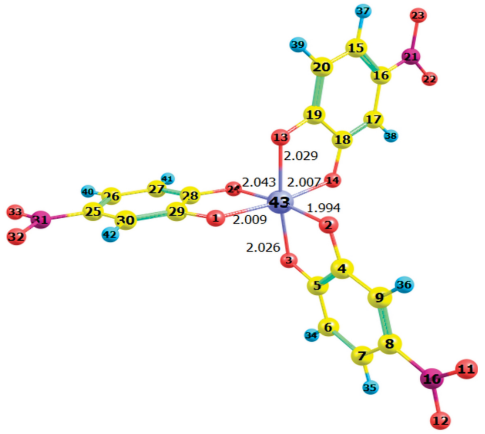

Figure 8. Ground-state equilibrium geometry of $[Cr(4NC)_3]^{3-}$ optimized at the B3LYP/6-311G level in the gas phase.

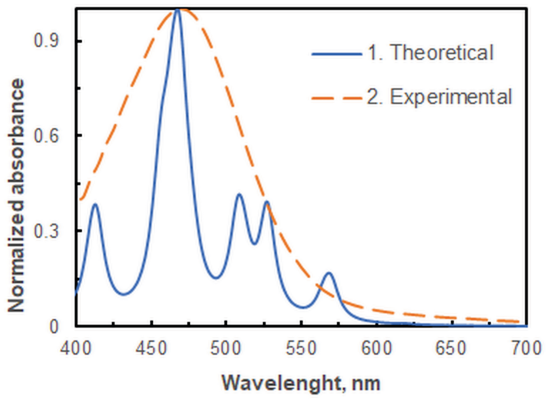

Figure 9. Comparison of the normalized experimental spectrum under optimum conditions and theoretical spectrum of the anionic structure from Figure 7. The theoretical spectrum was produced using a Lorentzian broadening and a scaling coefficient of 0.814.

As in the Fe(III) complex, the benzene rings of the 4NC ligands in $[Cr(4NC)_3]^{3-}$ retain their aromatic character. This is evidenced by the C–C bond lengths within the rings, which closely match those reported by Cornard et al.[65] for the free ligand (H_2L). Consequently, no quinoid distortions—characteristic of certain other catechol derivatives and detrimental to the complex's practical performance—are observed.

Figure 9 compares the normalized experimental spectrum of the extracted complex with the normalized theoretical spectrum of the anionic chromophore, $[Cr(4NC)_3]^{3-}$, obtained from calculated vertical excitation

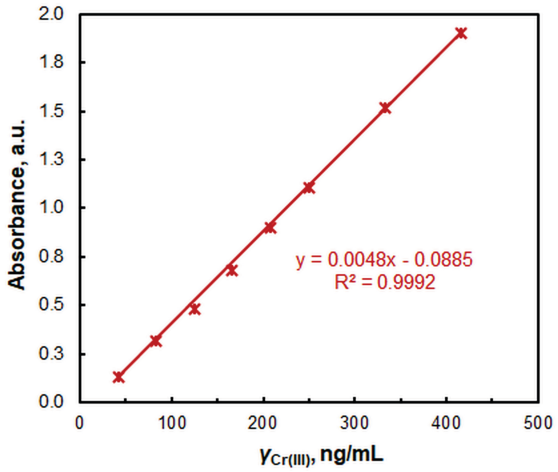

Figure 10. Calibration plot under the optimum conditions listed in Table 1.

energies. The two spectra agree very well, which provides independent support for the experimental determination of the complex's stoichiometry and complexation equation.

Calibration Plot, Preconcentration Factor, and Conditional Extraction Constant

The relationship between the measured absorbance (A) and Cr(III) concentration was linear within the range of 40–420 ng mL^{-1} Cr(III) (Figure 10). The linear regression equation was $A = 4.8 \times 10^{-3}\gamma - 0.089$, where γ is the concentration in ng mL^{-1}. The experimental setup involved approximately tenfold preconcentration, achieved with an aqueous phase volume of 50 mL and a diluted SRP volume of 5.06 mL (m = 5.00 g; ρ = 0.9877 g mL^{-1}). The apparent molar absorptivity was determined to be 2.4×10^5 M^{-1} cm^{-1}, and Sandell's sensitivity was 0.22 ng cm^{-2}.

The limit of detection (LOD) and limit of quantitation (LOQ), calculated as 3 σ and 10 σ of the blank absorbance (n = 10) divided by the slope, were 12 and 40 ng mL^{-1}, respectively.

The extraction constant (K_{ex}) characterizing Equation 1 was determined by both the mobile equilibrium method[63] (Figure 6) and the Holme–Langmyhr method.[69] The logarithmic values obtained by these methods were statistically identical: 12.2 ± 0.6 and 12.0 ± 0.1 (mean ± SD), respectively.

CONCLUSIONS

The formation of a ternary complex between Cr(III), 4NC, and A336 in a MM-CPE system was systematically investigated. The anionic component, $[Cr(4NC)_3]^{3-}$–responsible for the visible spectral bands (λ_{max} = 475 nm)–was further characterized by TD DFT calculations at the B3LYP/6 311G level. The close agreement between the calculated and experimental spectra validated the anticipated stoichiometry. The proposed novel CPE method aligns with modern trends, offering an environmentally friendly and cost-effective approach that requires neither sophisticated instrumentation nor expensive consumables. Notably, this work demonstrates for the first time that 4NC—a well-established analytical reagent—can serve effectively in the preconcentration of Cr(III).

Acknowledgment. The theoretical research was carried out using the infrastructure purchased under the National Roadmap for RI, financially coordinated by the MES of the Republic of Bulgaria (grant No D01-98/26.06.2025).

REFERENCES

1. IMA Mineral List with Database of Mineral Properties – Rruff, https://rruff.info/ima/, (accessed: October 22, 2025)
2. A. F. Burg, G. M. Hiedrich, A. B. Viana, V. L. Dressler, *Quím. Nova* **2024**, *48*, e-20250043. https://doi.org/10.21577/0100-4042.20250043
3. H. Haroon, T. A. Butt, J. A. Shah, A. Ciobica, L. E. Romila, V. Burlui, H. Bibi, M. Bilal, *Front. Chem.* **2025**, *13*, 1–25. https://doi.org/10.3389/fchem.2025.1608863
4. C. Khan, R. N. Malik, J. Chen, *Heliyon* **2024**, *10*, e40083. https://doi.org/10.1016/j.heliyon.2024.e40083
5. T. Ashfaq-Butt, *Croat. Chem. Acta* **2025**, *98*, 37–51. https://doi.org/10.5562/cca4096
6. J. B. Vincent, *Dalton Trans.* **2010**, *39*, 3787–3794. https://doi.org/10.1039/b920480f
7. A. Monga, A. B. Fulke, D. Dasgupta, *J. Hazard. Mater. Adv.* **2022**, *7*, 100113. https://doi.org/10.1016/j.hazadv.2022.100113
8. J. Dikobe, F. A. Melato, C. J. L. Adlem, K. Netshiongolwe, *Heliyon* **2024**, *10*, e34670. https://doi.org/10.1016/j.heliyon.2024.e34670
9. J. B. Vincent, S. Brown, in *The nutritional biochemistry of chromium(III)* (Ed.: J. B. Vincent), Elsevier, Netherlands, **2018**, pp. 1–60.
10. J. B. Vincent, *J. Nutr.* **2017**, *147*, 2212–2219. https://doi.org/10.3945/jn.117.255901
11. M. G. Arellano-Sánchez, C. Devouge-Boyer, M. Hubert-Roux, C. Afonso, M. Mignot, *Crit. Rev. Anal. Chem.* **2022**, *52*, 1537–1556 https://doi.org/10.1080/10408347.2021.1890545
12. EFSA Panel on Dietetic Products, Nutrition and Allergies, *EFSA J.* **2014**, *12*, 3845. https://doi.org/10.2903/j.efsa.2014.3845
13. J. Liang, X. Huang, J. Yan, Y. Li, Z. Zhao, Y. Liu, J. Ye, Y. Wei, *Sci. Total Environ.* **2021**, *774*, 145762. https://doi.org/10.1016/j.scitotenv.2021.145762

14. L. Ghezzi, E. Mugnaioli, N. Perchiazzi, C. Duce, C. Pelosi, E. Zamponi, S. Pollastri, B. Campanella, M. Onor, M. Abdellatief, F. Franceschini, R. Petrini, *Sci. Rep.* **2023**, *13*, 16283. https://doi.org/10.1038/s41598-023-43579-9
15. J. B. Vincent, *Met. Ions Life Sci.* **2013**, *13*, 171. https://doi.org/10.1007/978-94-007-7500-8_6
16. I. M. Shaker, A. F. Khudhair, H. H. Mihsen, *Baghdad Sci. J.* **2025**, *22*, 406–418. https://doi.org/10.21123/bsj.2024.9558
17. R. K. Mamedova, S. G. Aliyev, N. S. Hasanova, N. A. Verdizadeh, A. Z. Zalov, *Int. J. Chem. Stud.* **2017**, *5*, 1255–1262.
18. H. A. H. A. Ameer, A. F. Hussain, *Baghdad Sci. J.* **2023**, *20*, 1331. https://doi.org/10.21123/bsj.2023.7393
19. N. Dawra, N. Dabas, *Int. J. Environ. Anal. Chem.* **2024**, *104*, 2994–3015. https://doi.org/10.1080/03067319.2022.2076224
20. N. S. Hasanova, *Chem. Probl.* **2019**, *17*, 518. https://doi.org/10.32737/2221-8688-2019-4-518-525
21. A. Z. Zalov, S. A. Mammadova, N. S. Hasanova and S. A. Ibrahimova, *Chemical Problems* **2020**, *18*, 164. https://doi.org/10.32737/2221-8688-2020-2-164-173
22. L. S. d. Carvalho, A. C. S. Costa, S. L. Ferreira, L. S. Teixeira, *J. Braz. Chem. Soc.* **2004**, *15*, 153. https://doi.org/10.1590/S0103-50532004000100025
23. Y. Anjaneyulu, M. R. Reddy, C. S. Kavipurapu, *Analyst* **1986**, *111*, 1167–1169. https://doi.org/10.1039/AN9861101167
24. B. Subrahmanyam, M. Eshwar, *Microchim. Acta* **1976**, *66*, 579–584. https://doi.org/10.1007/BF01220116
25. T. N. Simonova, V. A. Dubrovina, A. B. Vishnikin, *J. Serb. Chem. Soc.* **2016**, *81*, 645–659. https://doi.org/10.2298/JSC150630016S
26. Z. Bahadir, V. N. Bulut, M. Hidalgo, M. Soylak, E. Marguí, *Spectroc. Acta Pt. B-Atom. Spectr.* **2016**, *115*, 46–51. https://doi.org/10.1016/j.sab.2015.11.001
27. H. Zhang, W. Wu, *Anal. Sci.* **2018**, *34*, 305–309. https://doi.org/10.2116/analsci.34.305
28. G. V. Rathaiah, M. C. Eshwar, *Bull. Chem. Soc. Jpn.* **2006**, *58*, 2447–2448. https://doi.org/10.1246/bcsj.58.2447
29. R. Halko, I. Hagarová, V. Andruch, *J. Chromatogr. A* **2023**, *1701*, 464053. https://doi.org/10.1016/j.chroma.2023.464053
30. W. I. Mortada, *Microchem. J.* **2020**, *157*, 105055. https://doi.org/10.1016/j.microc.2020.105055
31. P. Samaddar, K. Sen, *J. Ind. Eng. Chem.* **2014**, *20*, 1209–1219. https://doi.org/10.1016/j.jiec.2013.10.033
32. K. Pytlakowska, V. Kozik, M. Dabioch, *Talanta* **2013**, *110*, 202–228. https://doi.org/10.1016/j.talanta.2013.02.037
33. C. D. Stalikas, *Trac-Trends Anal. Chem.* **2002**, *21*, 343–355. https://doi.org/10.1016/S0165-9936(02)00502-2
34. K. M. Algheryani, A. A. Asweisi, *J. Eng. Ind. Res.* **2023**, *4*, 68–76. https://doi.org/10.48309/jeires.2023.2.1
35. E. K. Paleologos, C. D. Stalikas, S. M. Tzouwara-Karayanni, G. A. Pilidis, M. I. Karayannis, *J. Anal. At. Spectrom.* **2000**, *15*, 287–291. https://doi.org/10.1039/a908974h
36. E. K. Paleologos, C. D. Stalikas, S. M. Tzouwara-Karayanni, M. I. Karayannis, *Anal. Chim. Acta* **2001**, *436*, 49–57 https://doi.org/10.1016/S0003-2670(01)00884-4
37. P. Liang, J. Li, *Atom. Spectrosc.* **2005**, *26*, 89.
38. Y. Li, B. Hu, Z. Jiang, Y. Wu, *Anal. Lett.* **2006**, *39*, 809–822. https://doi.org/10.1080/00032710600611574
39. P. Liang, H. Sang, *J. Hazard. Mat.* **2008**, *154*, 1115–1119. https://doi.org/10.1016/j.jhazmat.2007.11.017
40. Z. Sun, P. Liang, *Microchim. Acta* **2008**, *162*, 121–125. https://doi.org/10.1007/s00604-007-0942-0
41. L. MacHáčková, M. Žemberyová, *Anal. Methods.* **2012**, *4*, 4042–4048. https://doi.org/10.1039/c2ay25831e
42. H. İ. Ulusoy, R. Gürkan, Ö. Yılmaz, M. Akçay, *J. Anal. Chem.* **2012**, *67*, 131–139. https://doi.org/10.1134/S1061934812020141
43. M. Sun, Q. Wu, *J. Pharm. Biomed. Anal.* **2012**, *60*, 14–18. https://doi.org/10.1016/j.jpba.2011.10.034
44. L. Zhang, X. Li, X. Wang, W. Wang, X. Wang, H. Han, *Anal. Methods* **2014**, *6*, 5578–5583. https://doi.org/10.1039/C4AY00922C
45. K. H. Kadhim, A. N. Alsharifi, A. S. Abbas, *Asian J. Chem.* **2014**, *26*, S139. https://doi.org/10.14233/ajchem.2014.19032
46. L. Meng, J. Ning, J. Zhao, L. Bi, *Asian J. Chem.* **2014**, *26*, 2483. https://doi.org/10.14233/ajchem.2014.16645
47. L. Meng, J. Ning, Y. Yang, *Water Sci. Technol.* **2014**, *70*, 1913–1918. https://doi.org/10.2166/wst.2014.412
48. I. López-García, Y. Vicente-Martínez, M. Hernández-Córdoba, *Talanta* **2015**, *132*, 23–28. https://doi.org/10.1016/j.talanta.2014.08.036
49. C. Wang, D. F. Martin, B. B. Martin, *J. Environ. Sci. Health Part A* **1998**, *33*, 1631–1642. https://doi.org/10.1080/10934529809376808
50. L. Sommer, G. Ackermann, D. T. Burns, S. B. Savvin, *Pure Appl. Chem.* **1990**, *62*, 2147–2166. https://doi.org/10.1351/pac199062112147
51. K. B. Gavazov, *Acta Chim. Slov.* **2012**, *59*, 1–17.
52. V. V. Divarova, K. T. Stojnova, I. D. Radkovska, A. D. Saravanska, G. K. Toncheva, V. B. Delchev, K. B. Gavazov, *Acta Chim. Slov.* **2024**, *71*, 519. https://doi.org/10.17344/acsi.2024.8835
53. P. V. Racheva, A. D. Saravanska, G. K. Toncheva, D. D. Kiradzhiyska, N. P. Milcheva, V. V. Divarova, I. P. Pencheva, K. T. Stojnova, V. B. Delchev, K. B. Gavazov, *Molecules* **2025**, *30*, 899. https://doi.org/10.3390/molecules30040899

54. Sigma-Aldrich safety data sheet. 4-Nitrocatechol, https://www.sigmaaldrich.com/BG/en/sds/aldrich/n15553, (accessed: September 14, 2025)
55. A. Gajdošová, P. Racheva, D. Kiradzhiyska, V. Divarova, A. Saravanska, J. Šandrejová, K. Gavazov, *Int. J. Mol. Sci.* **2025**, *26*, 5808. https://doi.org/10.3390/ijms26125808
56. V. Divarova, A. Gajdošová, P. Racheva, K. Gavazov, *Int. J. Mol. Sci.* **2025**, *26*, 4597. https://doi.org/10.3390/ijms26104597
57. D. Kiradzhiyska, N. Milcheva, M. Ruzmanova, F. Genç, P. Racheva, K. Gavazov, *Molecules* **2025**, *30*, 3287. https://doi.org/10.3390/molecules30153287
58. J.-P. Mikkola, P. Virtanen, R. Sjoholm, *Green Chem.* **2006**, *8*, 250–255. https://doi.org/10.1039/B512819F
59. D. S. Krishna, N. N. Meeravali, J. K. Sunil, *Int. J. Environ. Anal. Chem.* **2020**, *100*, 1079–1093. https://doi.org/10.1080/03067319.2019.1648643
60. Z. Marczenko, M. Balcerzak, *Separation, preconcentration and spectrophotometry in inorganic analysis*, Elsevier, Amsterdam, **2000**, pp.159–166.
61. Gaussian 16, M. J. Frisch, G. W. Trucks, H. B. Schlegel, G. E. Scuseria, M. A. Robb, J. R. Cheeseman, G. Scalmani, V. Barone, G. A. Petersson, H. Nakatsuji, X. Li, M. Caricato, A. V. Marenich, J. Bloino, B. G. Janesko, R. Gomperts, B. Mennucci, H. P. Hratchian, J. V. Ortiz, A. F. Izmaylov, J. L. Sonnenberg, F. D. Williams, F. Lipparini, F. Egidi, J. Goings, B. Peng, A. Petrone, T. Henderson, D. Ranasinghe, V. G. Zakrzewski, J. Gao, N. Rega, G. Zheng, W. Liang, M. Hada, M. Ehara, K. Toyota, R. Fukuda, J. Hasegawa, M. Ishida, T. Nakajima, Y. Honda, O. Kitao, H. Nakai, T. Vreven, K. Throssell, J. A. Montgomery Jr., J. E. Peralta, F. Ogliaro, M. J. Bearpark, J. J. Heyd, E. N. Brothers, K. N. Kudin, V. N. Staroverov, T. A. Keith, R. Kobayashi, J. Normand, K. Raghavachari, A. P. Rendell, J. C. Burant, S. S. Iyengar, J. Tomasi, M. Cossi, J. M. Millam, M. Klene, C. Adamo, R. Cammi, J. W. Ochterski, R. L. Martin, K. Morokuma, O. Farkas, J. B. Foresman and D. J. Fox, Gaussian, Inc., Wallingford CT, **2016**.
62. Chemcraft, v. 1.8, G. A. Andrienko, http://www.chemcraftprog.com (accessed: September 14, 2025)
63. Z. Zhiming, M. Dongsten, Y. Cunxiao, *J. Rare Earths* **1997**, *15*, 216–219.
64. V. M. Nurchi, T. Pivetta, J. I. Lachowicz, G. Crisponi, *J. Inorg. Biochem.* **2009**, *103*, 227–236. https://doi.org/10.1016/j.jinorgbio.2008.10.011
65. J.-P. Cornard, Rasmiwetti, J.-C. Merlin, *Chem. Phys.* **2005**, *309*, 239–249. https://doi.org/10.1016/j.chemphys.2004.09.020
66. V. V. Divarova, A. D. Saravanska, G. K. Toncheva, N. Milcheva, V. B. Delchev, K. B. Gavazov, *Molecules* **2022**, *27*, 1217. https://doi.org/10.3390/molecules27041217
67. A. D. Saravanska, P. V. Racheva, V. V. Divarova, G. K. Toncheva, N. P. Milcheva, V. B. Delchev, K. B. Gavazov, *Russ. J. Inorg. Chem.* **2021**, *66*, 1880–1886. https://doi.org/10.1134/S0036023621120147
68. P. V. Racheva, N. P. Milcheva, A. D. Saravanska, K. B. Gavazov, *Croat. Chem. Acta* **2020**, *93*, 159–165. https://doi.org/10.5562/cca3722
69. A. Holme, F. J. Langmyhr, *Anal. Chim. Acta* **1966**, *36*, 383–391. https://doi.org/10.1016/0003-2670(66)80066-1